Amorphization-induced strong localization of electronic states in $CsPbBr_3$ and $CsPbCl_3$ studied by optical absorption measurements

S. Kondo, T. Sakai, H. Tanaka, and T. Saito
Department of Applied Physics, Faculty of Engineering, Fukui University, Bunkyo, Fukui 910, Japan
(Received 22 December 1997)

Optical absorption spectra of amorphous $CsPbX_3$ films (X=Br,Cl) are characterized by two Gaussian bands near the fundamental edge, with the optical energy gap largely blueshifted and the absorption intensity strongly reduced as compared with the crystalline films. The peak energies of the bands are close to those of the A and C bands of Pb-doped alkali halides. The spectral features are discussed in terms of a molecular orbital theory based on a quasicomplex $Pb^{2+}(X^-)_6$ model similar to the complex model for the doped alkali halides. It is shown that not only Pb^{2+} $6s$ and $6p$ extended states near the band edges but also X^- p states contributing to upper valence bands are localized by amorphization. The transitions from the localized Pb^{2+} $6s$ to $6p$ states produce the spin-orbit allowed $^3P_1$ and dipole allowed $^1P_1$ states responsible for the two Gaussians. The localized X^- p states lie deeper in energy than the localized Pb^{2+} $6s$ state and only contribute to higher-energy absorption above the Gaussian bands, giving the reason for the reduced absorption near the fundamental edge. The blueshift of the optical energy gap is attributed to the disappearance of k dispersions for these one-electron states. [S0163-1829(98)06341-3]

I. INTRODUCTION

The Pb atoms in PbX_2 (X=I,Br,Cl,F) and $CsPbX_3$ (X=Br,Cl) make a dominant contribution to the optical properties of the compounds in the region near the optical energy gap. In PbX_2, all of which can be amorphized by quench deposition,[1–4] optical absorption near the fundamental edge is based on Pb $6s$ to $6p$ transitions exhibiting a sharp cationic exciton peak in the crystalline (c) state (PbI_2 is an extensively investigated material both experimentally[5] and theoretically,[6] though experimental studies have only been reported for $PbBr_2$,[7–11] and $PbCl_2$ (Refs. 7–9, 11, and 12); as to PbF_2 only a few, but both theoretical[13] and experimental,[9,14] works are available in literature). In the amorphous (a) state, their absorption spectra are classified according to the crystal structure into which the compounds crystallize. In a-PbI_2 (which crystallizes into a layer structure), no structure is observed near the fundamental edge,[1] while other a-PbX_2 with X=Br, Cl, and F (which crystallize into an orthorhombic structure) are characterized by a prominent first absorption band due to Pb $6s$ to $6p$ excitation.[2–4]

According to our line-shape analysis performed on the absorption spectra of amorphous lead halides,[15] a-PbI_2 is a typical material obeying the Tauc law, as in the case of ordinary covalent semiconductors. In contrast, the first band of a-PbX_2 with X=Br, Cl, and F is by no means fitted with any power law, but instead an excellent fit to the band is obtained with a Gaussian function. Such a distinct difference between PbI_2 and PbX_2 originates in the difference in their electronic energy band structure. The Gaussian band in a-PbX_2 is explained as being due to localized electronic transitions of nonexcitonic origin within Pb^{2+} ions affected by inhomogeneous, local electric fields in the disordered network. Based on the obtained fitting parameters, an ''ion-glass'' model has been introduced, in which each Pb^{2+} ion is surrounded by nine neighboring X^- ions without any well-defined site symmetry around it.

The compounds $CsPbX_3$ (X=Br,Cl) crystallize in a slightly distorted perovskite structure. Their optical properties are governed by the octahedral quasicomplex $Pb^{2+}(X^-)_6$ embedded in a simple cubic matrix of Cs^+ ions. The six X^- ions are located at the face-centered positions of the cube and the cation Pb^{2+} is at the cube center. Heidelich *et al.*[16] has calculated the band structure of the compounds based on an empirical linear combination of atomic orbitals (LCAO) method completely neglecting the electronic orbitals of cesium: Upper valence bands are constructed from the Pb^{2+} $6s$ and Br^- $4p$ or Cl^- $3p$ orbitals, and lower conduction bands from Pb^{2+} $6p$ orbitals; a cationic direct energy gap is located at the R point in the Brillouin zone due to positive and negative k dispersions of the uppermost valence and lowermost conduction bands, respectively, along the Γ-R direction. The low-energy optical absorption[16–18] and reflection[16,19–21] spectra, which are characterized by a sharp first exciton (R-point exciton) peak around 2.3 eV for $CsPbBr_3$ and 3.0 eV for $CsPbCl_3$, have indeed been well explained in the framework of this model.

The motivation of the present study is based on the assumption that the ion-glass model such as proposed for a-PbX_2 may also be applicable to a-$CsPbX_3$; in a-$CsPbX_3$, the optical absorption at low photon energies may be caused by the cationic electronic transitions within Pb^{2+} ions surrounded by ''six'' (instead of ''nine'' for a-PbX_2) neighboring X^- ions. It is expected that a distorted (due to amorphization) quasicomplex $Pb^{2+}(X^-)_6$ embedded in a disordered Cs^+-ion matrix leads to enhanced localization of the cationic electronic transitions (within the Pb^{2+} ion) due to intervening Cs^+ ions as compared to the case of a-PbX_2, since the electronic orbitals of cesium do not contribute to the electronic states near the band edges as stated above. Therefore, it is useful to investigate optical properties of a-$CsPbX_3$ for obtaining a further clue to the nature of the ion glass. In the present study, amorphous films have been ob-

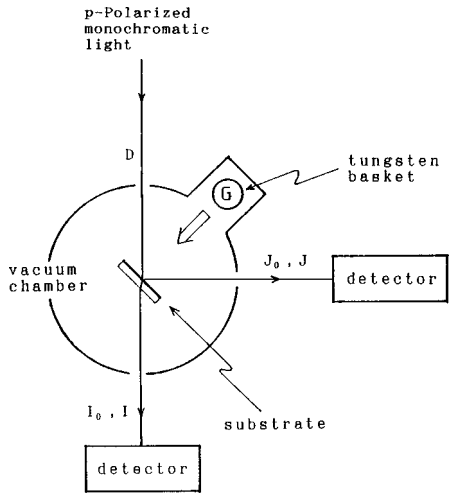

FIG. 1. The schematic view of the light path for *in situ* measurements of reflection-corrected OD spectra of a film quench deposited onto a cooled (to 77 K) substrate.

tained for $CsPbX_3$ by quench deposition, and their absorption spectra have been measured in the range up to 6.2 eV. Based on the line shape analysis of the spectra, we will give a thorough discussion of the nature of optical absorption and the related electronic state of a-$CsPbX_3$ including the comparison with the a-PbX_2 case.

II. EXPERIMENT

As starting materials CsX and PbX_2 (X=Br,Cl) of 99.9% purity were used. For the preparation of the compounds $CsPbX_3$, stoichiometric amounts of CsX and PbX_2 in powder form were thoroughly mixed together and molten for 15 min at 690 °C for X=Br and 600 °C for X=Cl in a silica-tube container purged with Ar gas. The container was then quenched in ice water to ensure homogeneity of the resulting compounds.

Simultaneous measurements of optical absorption and reflection were performed *in situ* on $CsPbX_3$ films quench deposited onto silica-glass substrates at 77 K at a rate of about 20 nm min^{-1}. The deposition was carried out in a vacuum of about 9×10^{-6} Pa using a tungsten basket heating element placed 8 cm in front of the substrate. The spectral measurements (resolution, 0.2 nm) were performed by a double-beam detection method, using a grating monochromator in combination with a 150-W xenon lamp as light source.

To measure absorption spectra accurately (for the purpose of performing the line-shape analysis of the resulting spectra), we employed an improved optical configuration shown in Fig. 1 (where the reference-light path in the double-beam detection method is omitted). The p-polarized monochromatic light is incident on the substrate at an incident angle of 45°. The optical density (OD) of the film was defined as

$$\mathrm{OD}=\log_{10}\frac{D-J}{I}-\log_{10}\frac{D-J_0}{I_0}, \tag{1}$$

where D is the intensity of the incident light, I_0 and J_0 are the intensities of transmitted and reflected light, respectively, from the substrate before the deposition of the film, and I and J are the corresponding light intensities after the film deposition. The first term in Eq. (1) corresponds to the optical density of the film-deposited substrate and the second term is the optical density of the substrate. Correction for reflectance at the film surfaces (both the substrate/film and vacuum/film interfaces) is involved in the first term. It is possible to represent Eq. (1) in terms of quantities independent of the characteristics of the two individual detectors (such as sensitivity, its wavelength dependence, etc.),

$$\mathrm{OD}=\log_{10}\frac{1-R_0R_r}{(1-R_0)T_r}, \tag{2}$$

where $T_r=I/I_0$, $R_r=J/J_0$, and R_0 is the reflectivity of the substrate. Then the values of OD can be determined from the measurements of the intensity ratios (T_r and R_r) of the light beams irradiating the individual detectors before and after the film deposition, using the predetermined values of R_0. The OD values thus determined are expected to be very accurate, since the optical configuration is kept unchanged throughout all the measurements and since all the imbalances in intensity between the probing and reference light are cancelled out.

The substrate (silica glass with 1 mm thickness) was put on a copper sample holder with a square light path 4×4 mm^2, attached to the bottom of a copper vessel in a cryostat. The vessel was filled with liquid nitrogen, or heated with a heater to control the temperature of the substrate. This permits us to measure *in situ* OD spectra for both the amorphous and crystalline phases of the same film and the crystallization temperature as well.

III. RESULTS

In Fig. 2 we compare the fundamental absorption spectra of a quench-deposited $CsPbBr_3$ film (upper half) with those of a quench-deposited $PbBr_2$ film (lower half, from Ref. 2). Spectra 1 were first measured at 77 K for the as-deposited films. Then the films were annealed for 10 min at 500 K for $CsPbBr_3$ and 400 K for $PbBr_2$, and cooled again to 77 K to measure spectra 2. The as-deposited $PbBr_2$ film is in the amorphous state and the annealed one is in the crystalline state.[2] In $CsPbBr_3$, spectrum 1 is composed of two broad bands peaking at 3.87 and 5.23 eV. By annealing the film, a sharp excitonic peak shows up at 2.357 eV characteristic of crystalline $CsPbBr_3$,[21] as seen from spectrum 2. It should be noted here that the as-deposited film exhibits a strongly reduced optical absorption in comparison to the annealed film. Furthermore, spectrum 1 has about a 1 eV larger optical energy gap than spectrum 2. It is interesting to note that the as-deposited $CsPbBr_3$ film has almost the same optical energy gap (about 3.5 eV) as that of the a-$PbBr_2$ film, despite the large difference in the gap after annealing the films.

Figure 3 shows the change in transmittance at 3.26 eV during heating of a $CsPbBr_3$ film. In the measurement, the as-deposited film was heated at a rate of 1 K min^{-1} up to 500 K (curve 1) and then the film was immediately cooled to 77 K at a rate of 10 K min^{-1} to measure the second curve (curve 2) at the same heating rate. Curve 1 clearly shows a drastic change (decrease) in the transmittance in a narrow temperature range of 4 K near 298 K, while curve 2 no longer exhibits such a marked change and was shown to be

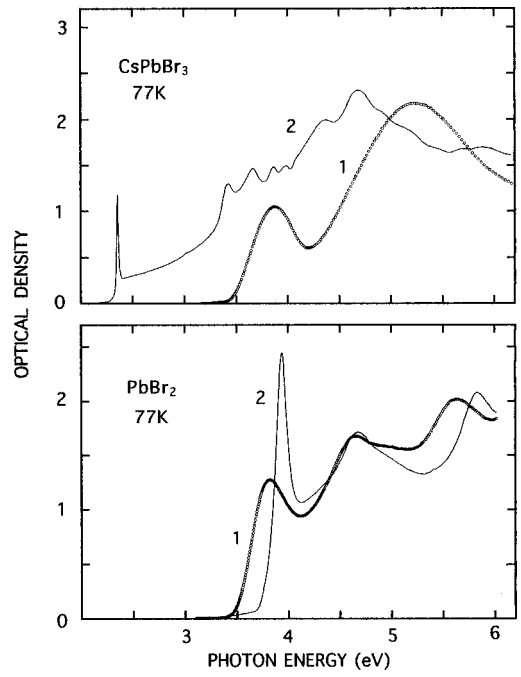

FIG. 2. Comparison of fundamental absorption spectra of a quench-deposited film of $CsPbBr_3$ (upper half) to those of $PbBr_2$ (lower half, from Ref. 2), measured at 77 K for the as-deposited (amorphous, 1) and annealed (crystalline, 2) films.

reversible (below 500 K) by measuring a third curve. The drastic change in curve 1 is very similar in sharpness to previous results on a-$PbBr_2$,[2] and provides evidence of a well-defined phase transition from amorphous to crystalline states in the quench-deposited $CsPbBr_3$ film, though structural studies are necessary for a direct support. (It has been reported for a ternary Ge-Sb-Te solid solution, which is a promising material for fast phase-change optical disks,[22,23] that an abrupt transmittance change during slow heating of the amorphous film is due to nucleation followed by a fast grain-growth process resulting in a crystalline film.[24]) The transition temperature (crystallization temperature, T_c), which we defined here as the onset temperature for the drastic change, was 296 K as compared with 335 K for $PbBr_2$. The irreversible change just above the drastic change (300–420 K in curve 1) is considered to be due to crystal growth in the film.

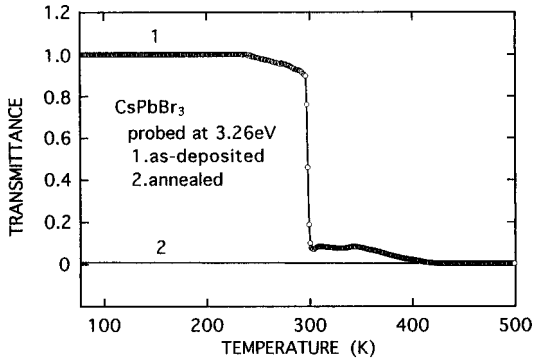

FIG. 3. The change in transmittance at photon energy 3.26 eV during heating (1 K min^{-1}), measured for the first (1) and second (2) heating cycles of a quench-deposited $CsPbBr_3$ film.

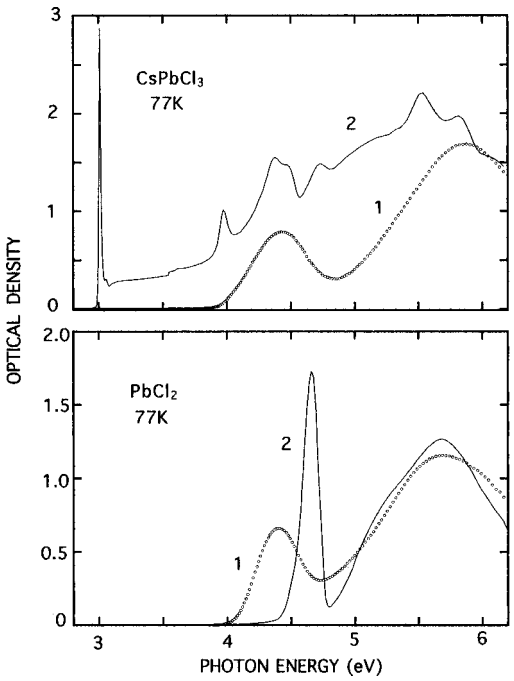

FIG. 4. Comparison of fundamental absorption spectra of a quench-deposited film of $CsPbCl_3$ (upper half) to those of $PbCl_2$ (lower half, from Ref. 3), measured at 77 K for the as-deposited (amorphous, 1) and annealed (crystalline, 2) films.

Such a drastic change in transmittance as above was also observed for a-$CsPbCl_3$, leading to a crystallization temperature of 302 K, very close to that of a-$CsPbBr_3$ in contrast to the considerably lower crystallization temperature for $PbCl_2$, 281.5 K,[3] than for $PbBr_2$.

Figure 4 is a comparison of the fundamental absorption spectra of a quench-deposited $CsPbCl_3$ film (upper half) with those of a quench-deposited $PbCl_2$ film (lower half, from Ref. 3) in their amorphous (spectra 1) and crystalline (spectra 2) states. These spectra were obtained in the same way as those of the bromides but with an annealing temperature of 400 K for both $CsPbCl_3$ and $PbCl_2$. As in the case of the bromides, the spectrum of a-$CsPbCl_3$ is composed of two broad bands with the peaks at 4.43 and 5.88 eV and exhibits nearly the same optical energy gap (about 4 eV) as that of a-$PbCl_2$; the amorphization is again characterized by a large blueshift (about 1 eV) of the fundamental edge and significant reduction in the absorption intensity; after crystallization, a very sharp exciton peak appears at 3.013 eV.

It is worth noting that the full widths at half maximum (FWHM's) of the exciton peaks, 15 meV for c-$CsPbBr_3$ and 14 meV for c-$CsPbCl_3$, are comparable to that of the reflection spectrum at 4.2 K of a single crystal of $CsPbCl_3$, 12 meV,[21] and are much smaller than those of the ''improved'' films in Ref. 18 (where the FWHM's are, though not explicitly given, of the order of 30 meV for both of the $CsPbBr_3$ and $CsPbCl_3$ films as are read from the presented spectra at 77 K). This suggests that the process of amorphization and subsequent heat treatment (annealing) is favorable for achieving high-quality polycrystalline films free from strains and lattice defects.

IV. DISCUSSION

It has been shown[15] that the first absorption bands of a-PbX_2 (X=Br,Cl,F) are well fitted to single Gaussian func-

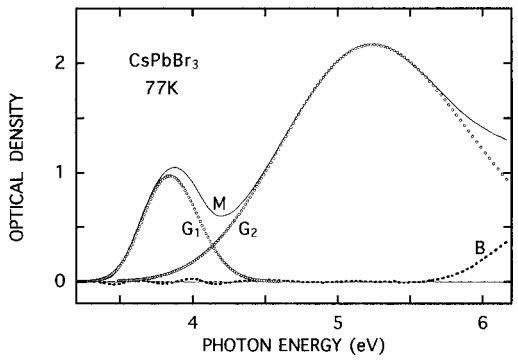

FIG. 5. Line-shape analysis of the absorption spectrum of a-$CsPbBr_3$. The measured spectrum (M) is decomposed into two Gaussian bands, the low- (G_1) and high- (G_2) energy components, with the remainder (M minus G_1 minus G_2) as the background absorption (B).

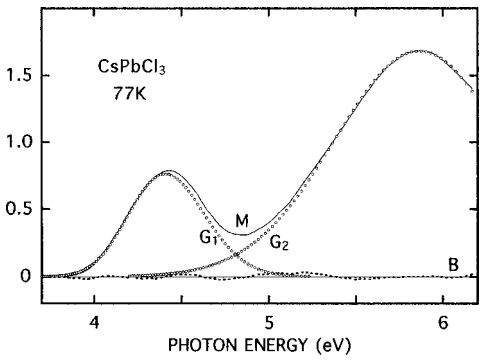

FIG. 6. Line-shape analysis of the absorption spectrum (M) of a-$CsPbCl_3$ similar to that for $CsPbBr_3$, with the same notations for the resulting curves as in Fig. 5.

tions, as compared to the c-phase excitonic absorption bands fitted to multiple Lorentzian functions. As mentioned in Sec. I, the fitting parameters for the Gaussian bands have led to an ''ion-glass'' model for the amorphous state, in which each individual Pb^{2+} ion is surrounded (and thus localized) by nine negative ions forming the quasicomplex $Pb^{2+}(X^-)_9$ without any well-defined site symmetry around the central Pb^{2+} ion.

In a-$CsPbX_3$ (X=Br,Cl), the absorption spectra are composed of two broad bands (Figs. 2 and 4), and it is possible to decompose the spectra into two Gaussian functions. The results are shown in Figs. 5 and 6. In both figures, the measured spectra (curves M) are nicely decomposed into two Gaussian bands (curves G_1 and G_2); the difference in intensity between the measured spectrum and the total intensities of the two Gaussian bands (M minus G_1 minus G_2, curves B) is, indeed, almost zero in the photon energy region up to 5.7 eV for a-$CsPbBr_3$ (Fig. 5) and in the whole measurement range for a-$CsPbCl_3$ (Fig. 6). The peak energies (E_1,E_2) and FWHM's (Γ_1,Γ_2) of the respective Gaussian bands are listed in Table I together with the peak energy difference (E_2-E_1). For comparison, the corresponding values of the first Gaussian bands previously obtained[15] for a-$PbBr_2$ and a-$PbCl_2$ are also listed in the table.

It is noted that a-$CsPbX_3$ and a-PbX_2 have similar values of E_1 and Γ_1 in both halides (X=Br,Cl). This indicates that, in analogy with the case of a-PbX_2, the first absorption bands of a-$CsPbX_3$ arise from localized, cationic electronic transitions within Pb^{2+} ions surrounded by six (instead of nine for a-PbX_2) X^- ions; these ions, forming quasicomplexes $Pb^{2+}(X^-)_6$ without any well-defined site symmetry around the central Pb^{2+} ion, are embedded in a disordered Cs^+-ion network. The small differences in magnitude of the fitting parameters between a-$CsPbX_3$ and a-PbX_2 are considered to be due to the difference in the coordination number of the quasicomplexes.

A more noticeable result of the spectral decomposition is that, in contrast to the case of a-PbX_2, not only the first absorption bands but also the second bands of a-$CsPbX_3$ are well fitted to the Gaussian functions. Therefore, it is plausible to relate both bands to localized excitations of Pb^{2+} ions. We note here that the values of E_2-E_1, 1.398 eV for a-$CsPbBr_3$ and 1.460 eV for $CsPbCl_3$, are comparable to the Pb $6p$ spin-orbit splitting energy, 1.3 eV.[6]

It is instructive to compare the spectra of a-$CsPbX_3$ with the absorption spectra[25,26] of Pb-doped CsX crystal (X=Br,Cl). According to Ref. 25, the latter spectra (at room temperature) are composed of two Gaussian bands termed A and C, with a vibration-induced weak subband B between them. The energy locations (E_A,E_C) and FWHM's (Γ_A,Γ_C) of the main bands A and C are listed in Table II together with the peak-energy difference (E_C-E_A). The two bands A and C are known to be due to the spin-orbit allowed $^1S_0 \rightarrow {}^3P_1$ and the dipole allowed $^1S_0 \rightarrow {}^1P_1$ transitions, respectively, in the Pb^{2+} ion. As seen from the comparison of Tables I and II, there exists a close similarity between the values of E_A and E_1 for both bromides and chlorides. Furthermore, the values of E_C-E_A, which are mainly determined from the strength of spin-orbit interaction of the Pb $6p$ electron, are relatively close to those of E_2-E_1 in both cases of X=Br and Cl. Therefore, it is useful to discuss the G_1 and G_2 bands of a-$CsPbX_3$ on the basis of the physical model applied to the doped alkali halides. (There is no large difference in the absorption feature between Pb-doped ce-

TABLE I. The peak energies (E_1,E_2), their difference (E_2-E_1), and FWHM's (Γ_1,Γ_2) of the Gaussian bands (G_1,G_2) of a-$CsPbX_3$ for X=Br and Cl in unit of eV. Corresponding values of the first Gaussian bands of PbX_2 from Ref. 15 are also listed.

	E_1	E_2	E_2-E_1	Γ_1	Γ_2
a-$CsPbBr_3$	3.843	5.241	1.398	0.444	1.533
a-$PbBr_2$	3.700			0.400	
a-$CsPbCl_3$	4.406	5.866	1.460	0.510	1.138
a-$PbCl_2$	4.418			0.410	

TABLE II. The peak energies (E_A,E_C), their differences (E_C-E_A), and FWHM's (Γ_A,Γ_C) of the A and C absorption bands of Pb^{2+}-doped CsX single crystals for X=Br and Cl in units of eV, from Ref. 25.

	E_A	E_C	E_C-E_A	Γ_A	Γ_C
CaBr:Pb^{2+}	4.00	5.64	1.64	0.32	0.54
CsCl:Pb^{2+}	4.46	6.20	1.74	0.34	0.57

sium halides with bcc lattice and other Pb-doped alkali halides with fcc lattice, as exemplified in Ref. 25.)

Generally, the absorption spectra of s^2-configuration ions doped in alkali halides are interpreted in terms of a molecular orbital theory based on a complex model. Bramanti *et al.*[27] have performed molecular orbital calculations for T1-doped KCl based on an octahedral $T1^+(Cl^-)_6$ complex model. Following their model, we take into account the $6s$ and $6p$ orbitals of the central Pb^{2+} ion and the $4p$ or $3p$ orbitals of the X^- ion to construct molecular orbitals of the $Pb^{2+}(X^-)_6$ quasicomplex. From the transformation properties of these atomic orbitals in the O_h point group (a_{1g} for $6s$; t_{1u} for $6p$; a_{1g}, e_g, and t_{1u} for $4p\sigma$ or $3p\sigma$; t_{1u}, t_{1g}, t_{2u}, and t_{2g} for $4p\pi$ or $3p\pi$), there arise one occupied antibonding (a^a_{1g}), two occupied bonding ($2t^b_{1g}$), three occupied nonbonding (e^n_g,t^n_{2u}, and t^n_{2g}), and one unoccupied antibonding (t^a_{1u}) molecular orbitals. The transition from a^a_{1g} to t^a_{1u} produces two allowed states $^3T_{1u}$ and $^1T_{1u}$, which are responsible for the *A* and *C* bands, respectively, of the doped alkali halides. In the case of Pb-doped alkali halides, it has been shown from an f-sum measurement[28] of the *A*, *B*, and *C* bands that the contribution of the halogen p states to the highest occupied a^a_{1g} orbital (as well as to the unoccupied t^a_{1u} orbital) is very small (therefore, the $^3T_{1u}$ and $^1T_{1u}$ states are denoted as $^3P_1$ and $^1P_1$, respectively). This is favorable for relating the G_1 and G_2 bands of a-$CsPbX_3$ to excitation (to $^3P_1$ and $^1P_1$ states, respectively) of the central Pb^{2+} ion in the $Pb^{2+}(X^-)_6$ quasicomplex; the contribution of halogen p orbitals to these bands is considered to be negligible. We note that, in the Pb-doped alkali halides, a higher-energy absorption band, namely, the *D* band, has been assigned[29,30] as due to charge-transfer transitions from e^n_g to t^a_{1u} (e^n_g is the second-highest occupied orbital).

As is well known, valence and conduction bands in semiconductors retain their meaning even in the amorphous state. However, a certain amount of the extended states near the band edges are localized by amorphization. The first absorption bands of a-PbX_2 (X=Br,Cl) have indeed been related to electronic transitions between localized states,[15] i.e., from the filled localized states just above the mobility edge of the valence band to the empty ones just below the conduction mobility edge. The transitions are spatially allowed because the uppermost valence and the lowest conduction bands are both cationic (Pb^{2+} $6s$- and $6p$-like, respectively); the oscillatorlike character of the first band is attributed to the high densities of the localized states due to a relatively flat band structure of PbX_2. Furthermore, it has been shown[31] from an ''f-sum rule,'' applied to the Gaussian function for the first band in the a phase and the multiple Lorentzian functions for the excitonic absorption band in the c phase, that, by amorphization, all the extended states contributing to the c-phase excitonic transitions are localized and take part in the localized absorption responsible for the Gaussian band. It is therefore plausible to assume that the high-energy absorption above the first band of a-PbX_2 corresponds to transitions related to extended states (Pb $6s$-like localized to Pb $6p$-like extended, Pb $6s$-like extended to Pb $6p$-like localized, and/or Pb $6s$-like extended to Pb $6p$-like extended states, with a certain contribution of X $4p$- or $3p$-like extended states to the transitions as well). Indeed, the c-phase absorption spectra in the region above the excitonic transition energies exhibit similar features in outline to the a-phase ones in the same energy region as seen in Figs. 2 and 4 (lower halves).

In contrast, in $CsPbX_3$ (X=Br,Cl), there occurs a noticeable change in spectral shape by amorphization (Figs. 2 and 4, upper halves): i.e., the large blueshift ($\sim$1 eV) of the fundamental edge and significant reduction in the integrated absorption intensity (by a factor of $\sim$1.6 for X=Br and $\sim$2 for X=Cl in the measured region), giving rise to the two-Gaussians shape for the spectra. In terms of energy band structure, these features may be explained as follows.

As mentioned in Sec. I, the optical properties of c-$CsPbX_3$ are governed by the octahedral $Pb^{2+}(X^-)_6$ quasicomplex (embedded in a simple cubic Cs^+-ion matrix): The band structure calculation[16] based on an LCAO method indeed shows that upper valence bands are constructed from the Pb^{2+} $6s$ and X^- $4p$ or $3p$ orbitals, and lower conduction bands from Pb^{2+} $6p$ orbitals; the low-energy absorption spectra of c-$CsPbX_3$ are well interpreted in the framework of this band structure. In the present application (both the c and a phases), however, a convenient approach to the band structure may be provided by an LCMO (linear combination of molecular orbitals) method based on the quasicomplex as expected, though it is essentially the same as the LCAO method.

In the LCMO method, as suggested from the molecular orbital theory for the doped alkali halides mentioned above, upper valence bands of c-$CsPbX_3$ may be constructed from the a^a_{1g} and e^n_g orbitals, and lower conduction bands from the t^a_{1u} orbitals. Other molecular orbitals may only contribute to much deeper valence bands in energy. The cationic nature of the (R-point) exciton transition (the LCAO result[16]) is compatible with the transition from a^a_{1g}-like valence to t^a_{1u}-like conduction bands, since there is almost no contribution of halogen p orbitals to the a^a_{1g} and t^a_{1u} orbitals. Charge transfer transition is also expected to occur near the fundamental edge, owing to (positive) k dispersion for the e^n_g-orbital energy (of the upper valence bands) due to making extended states. By amorphization, however, there occurs significant change in the energy band as suggested from the spectral change. Both the conduction states coming from t^a_{1u} and the valence states coming from a^a_{1g} and e^n_g are considered to converge to their own localized states with particular eigenenergies. The resulting one-electron localized states may be of spin-orbit split Γ^-_6 (j=1/2) and Γ^-_8 (j=3/2) characters for t^a_{1u} and of Γ^+_6 (j=1/2) character for a^a_{1g} in the double-group notation for O_h, since then it is possible to produce the spin-orbit allowed $^3P_1$ state and the dipole allowed $^1P_1$ state responsible for the G_1 and G_2 bands, respectively, from the transitions $\Gamma^+_6 \rightarrow \Gamma^-_6$ and $\Gamma^+_6 \rightarrow \Gamma^-_8$, in the limit of the Russell-Saunders coupling. (Strictly speaking, the O_h symmetry of the $Pb^{2+}(X^-)_6$ quasicomplex is not well defined in the a phase.) On the other hand, the e^n_g localized states are, like the molecular orbital case for Pb-doped alkali halides, expected to lie deeper in energy than the Γ^+_6 (or a^a_{1g}) localized state, and thus their contribution to the absorption spectra (due to transitions to the Γ^-_6 and Γ^-_8 localized states) may occur at high energies above the G_1 and G_2 bands. This is favorable for explaining the signifi-

cantly reduced absorption intensity in the measurement energy region, below 6.2 eV. Due to such strong localizations of the one-electron states as above, the positive and negative k dispersions that exist in the c phase of the uppermost valence and lowermost conduction bands, respectively, along the Γ-R direction in the Brillouin zone, which is responsible for the very small optical energy gap (as well as for the R-point exciton absorption) in the c phase, may disappear (the quantity k is no longer well defined for localized states), resulting in the absence of low-energy absorption. This accounts for the large blueshift of the optical energy gap.

V. CONCLUSION

We have obtained amorphous films of $CsPbX_3$ (X=Br,Cl) by quench deposition onto 77-K substrates. Upon slow heating they show sharp crystallization behavior in a narrow temperature range, exhibiting a well-defined crystallization temperature of 296 K for $CsPbBr_3$ and 302 K for $CsPbCl_3$. The UV absorption spectra of a-$CsPbX_3$ are composed of two broad bands (first and second bands). The first bands are very similar in shape and energy location to the first absorption bands of respective a-PbX_2 resulting in nearly equal optical energy gaps between a-$CsPbX_3$ and a-PbX_2. It is shown that in a a-$CsPbX_3$ the spectra are nicely decomposed into two Gaussian functions, as compared to the case of a-PbX_2, where a nice fit to a Gaussian function is obtained for the first band, but not for the higher-energy bands. Further, there exist a noticeable spectral difference between the c- and a-$CsPbX_3$ in contrast to the case of PbX_2, i.e., the amorphization-induced large ($\sim$1 eV) blueshift of the fundamental edge and significant reduction of the integrated absorption intensity (by a factor of about 1.6 for $CsPbBr_3$ and about 2 for $CsPbCl_3$ in the measured region).

The peak energies of the first and second Gaussians of a-$CsPbX_3$ are close to those of the A and C bands of Pb-doped CsX crystals, respectively. For this reason, an LCMO band-structure approach starting from the molecular orbitals of the $Pb^{2+}(X^-)_6$ quasicomplex similar to the complex model for the doped alkali halides is used to explain the spectral change due to amorphization: By amorphization, both the conduction states coming from t_{1u}^a and the valence states coming from a_{1g}^a and e_g^n converge to their own localized states with particular eigenenergies. As a result, the optical absorption associated with the a_{1g}^a to t_{1u}^a transitions is changed to two discrete absorptions arising from the transitions from the $6s$ localized state to the spin-orbit split $6p_{1/2}$ and $6p_{3/2}$ localized states of the Pb^{2+} ion, responsible for the first and second Gaussians, respectively. The e_g^n localized states, lying deeper in energy than the Pb^{2+} $6s$ localized state, are considered to contribute to higher-energy optical absorption above the G_1 and G_2 bands. This accounts for the reduction of the integrated absorption intensity. On the other hand, the blueshift of the optical energy gap is attributed to the disappearance of k dispersions for these one-electron states.

These considerations are based on an ''ion-glass'' model, in which quasicomplexes $Pb^{2+}(X^-)_6$ without well-defined site symmetry around the central Pb^{2+} ion are embedded in a disordered Cs^+-ion matrix, with the Pb^{2+}-ion excitation energies strongly perturbed (Stark effect) in different ways due to different microscopic environments in the individual quasicomplexes. Here the intervening (between Pb^{2+} ions) Cs^+ ions act as the cause for the stronger electronic-state localization for a-$CsPbX_3$ than for a-PbX_2.

ACKNOWLEDGMENTS

This work was partly supported by The Hokuriku Industrial Advancement Center and partly by a Grant-in-Aid for Scientific Research from the Ministry of Education, Science, Sports and Culture in Japan.

[1] S. Kondo, M. Shiraki, and T. Saito, Jpn. J. Appl. Phys., Part 1 **31**, 3399 (1992).
[2] S. Kondo, T. Arakawa, and T. Saito, Jpn. J. Appl. Phys., Part 1 **32**, 4511 (1993).
[3] S. Kondo, H. Maruyama, and T. Saito, Phys. Status Solidi A **147**, 453 (1995).
[4] S. Kondo, M. Itoh, and T. Saito, Phys. Status Solidi A **154**, 591 (1996).
[5] For example, Le Chi Thanh, C. Depeursinge, F. Levy, and E. Mooser, J. Phys. Chem. Solids **36**, 699 (1975).
[6] For example, I. Ch. Schlüter and M. Schlüter, Phys. Rev. B **9**, 1652 (1974).
[7] W. C. De Gruijter, J. Solid State Chem. **6**, 151 (1973).
[8] A. F. Malysheva and V. G. Plekhanov, Opt. Spectrosc. **34**, 302 (1973).
[9] V. G. Plekhanov, Phys. Status Solidi B **57**, K55 (1973).
[10] A. J. H. EIjkelenkamp and K. Vos, Phys. Status Solidi B **76**, 769 (1976).
[11] M. Fujita, H. Nakagawa, K. Fukui, H. Matsumoto, T. Miyanaga, and M. Watanabe, J. Phys. Soc. Jpn. **60**, 4393 (1991).
[12] J. Kanbe, H. Takezoe, and R. Onaka, J. Phys. Soc. Jpn. **41**, 942 (1976).
[13] B. Velicky and J. Masek, Solid State Commun. **58**, 663 (1986).
[14] D. L. Alov and S. I. Rybchenko, J. Phys.: Condens. Matter **7**, 1475 (1995).
[15] S. Kondo, Phys. Status Solidi A **153**, 529 (1996).
[16] K. Heidelich, H. Kunzel, and J. Treusch, Solid State Commun. **25**, 887 (1978).
[17] H. Ito, H. Onuki, and R. Onaka, J. Phys. Soc. Jpn. **45**, 2043 (1978).
[18] D. Fröhlich, K. Heiderich, H. Kunzel, G. Trendel, and J. Treush, J. Lumin. **18/19**, 385 (1979).
[19] B. A. Belikovich, I. P. Pashchuk, and N. S. Pidzyrailo, Opt. Spectrosc. **42**, 62 (1977).
[20] L. N. Amitin, A. T. Anistratov, and A. I. Kuznetsov, Sov. Phys. Solid State **21**, 2041 (1979).
[21] I. P. Pashuk, N. S. Pidzyrailo, and M. G. Matsko, Sov. Phys. Solid State **23**, 1263 (1981).
[22] J. H. Coombs, A. P. J. M. Jongenelis, W. Van Es-Spiekman, and B. A. J. Jacobs, J. Appl. Phys. **78**, 4906 (1995).
[23] J. H. Coombs, A. P. J. M. Jongenelis, W. Van Es-Spiekman, and B. A. J. Jacobs, J. Appl. Phys. **78**, 4918 (1995).
[24] N. Ohshima, J. Appl. Phys. **79**, 8357 (1996).

[25] S. Radhakrishna and K. P. Pande, Phys. Rev. B **7**, 424 (1973).
[26] M. Nikl, K. Nitsch, and K. Polak, Phys. Rev. B **51**, 5192 (1995).
[27] D. Bramanti, M. Mancini, and A. Ranfagni, Phys. Rev. B **3**, 3670 (1971).
[28] P. R. Collins and W. J. Fredericks, J. Phys. Chem. Solids **47**, 529 (1986).
[29] T. Tsuboi, Physica B **96**, 341 (1979).
[30] S. Hashimoto and Y. Ohiwa, J. Phys. Soc. Jpn. **48**, 1655 (1980).
[31] S. Kondo, H. Maruyama, and T. Saito, Phys. Status Solidi A **158**, 529 (1996).